NATIONAL ADVISORY COMMITTEE FOR AERONAUTICS

TECHNICAL NOTE 2518

CRITERIONS FOR CONDENSATION-FREE FLOW IN SUPERSONIC TUNNELS

By Warren C. Burgess, Jr., and Ferris L. Seashore

Lewis Flight Propulsion Laboratory
Cleveland, Ohio

Washington
December 1951

NATIONAL ADVISORY COMMITTEE FOR AERONAUTICS

TECHNICAL NOTE 2518

CRITERIONS FOR CONDENSATION-FREE FLOW IN SUPERSONIC TUNNELS

By Warren C. Burgess, Jr. and Ferris L. Seashore

SUMMARY

The results of an investigation of water-vapor condensation shocks in the air passing through supersonic tunnels are presented. Criterions for condensation-free flow are established by correlating experimental observations with the Volmer theory of nuclei formation. Experimental observations were made at Mach numbers up to 2.01. The criterions are presented in a form independent of tunnel-inlet stagnation pressure and are extended theoretically to a Mach number of 4.00. Preliminary evidence of the effect of tunnel size on the criterions is presented.

INTRODUCTION

When a mixture of water vapor and air is expanded beyond saturation conditions in passing through a supersonic wind tunnel, a change of phase of the vapor resulting in a nonisentropic discontinuity of the flow is often observed. The discontinuity is referred to as a "condensation shock." Condensation shock, as used herein, however, refers only to that region of the air stream in which the increase in static pressure accompanying phase transition of the water vapor is measurable.

The change in static-pressure distribution, if it occurs in the nozzle of a supersonic tunnel, is indicative of a deviation from the ordered expansion of the flow. The design of the ensuing part of the nozzle is thereby invalidated and nonparallel flow exists at the nozzle outlet. Nonparallel-flow affects, accompanying condensation shocks, have been proven to complicate the interpretation of aerodynamic data (reference 1).

A theory for the formation of condensation nuclei that appears to be applicable to the treatment of condensation shocks is presented by Volmer in reference 2. This theory is modified herein and used in conjunction with experimental investigations made at

the NACA Lewis laboratory in order to establish criterions for condensation-free flow. The criterions are presented in a form independent of tunnel-inlet stagnation pressure. The physical phenomena related to the condensation are briefly discussed.

ANALYSIS

The partial pressure of a vapor p_v expanded through a supersonic tunnel may be assumed to change in accordance with the adiabatic gas law. The saturation-vapor pressure p_∞, however, may be assumed to change in accordance with the Clausius-Clapeyron relation. During expansion of the air through a tunnel, the partial pressure of the vapor therefore decreases as a power function of the temperature, whereas the saturation-vapor pressure decreases as an exponential function of the temperature. Thus, with adiabatic expansion, the partial pressure of the vapor may exceed the saturation-vapor pressure; that is, $p_v/p_\infty > 1$, which results in a supersaturation of vapor for a given temperature. This condition may be relieved by the transformation of the excess vapor into the liquid phase as droplets.

A requisite for the formation of droplets is nuclei upon which vapor can condense. A common source of nuclei may be the hygroscopic substances in the atmosphere. In a supersonic tunnel, however, the amount of vapor condensing on such available nuclei during their rapid passage through the tunnel was calculated to be negligible by Oswatitsch (reference 3). Condensation of water vapor in the absence of foreign nuclei has been observed with the Wilson cloud chamber (reference 4). In this reference it has been postulated that aggregates of water molecules form the required condensation nuclei. Because heavy condensation shocks have often been observed in supersonic tunnels, nuclei of this type may be assumed to exist at, or just prior to, the condensation shock.

In a system where aggregates of water molecules are continually forming and breaking up, an aggregate continually grows if the vapor pressure at the surface of the aggregate is less than the partial pressure of the vapor in the surrounding atmosphere. At equilibrium the radius of the droplet is defined in terms of the partial pressure of the vapor and the saturation-vapor pressure by the Thomson relation (reference 2, p. 19):

$$r = \frac{2S}{\rho_l} \frac{m}{Rt} \frac{1}{\log_e (p_v/p_\infty)} \tag{1}$$

where

r radius of aggregate, centimeters

S surface tension of liquid, dynes/centimeters

ρ_l density of liquid, grams/cubic centimeter

m molecular weight of vapor, grams/mole

R universal gas constant, joules/(^{o}C)(mole)

t absolute temperature, ^{o}K

p_v/p_∞ ratio of partial pressure of vapor to saturation-vapor pressure in equilibrium with infinite liquid surface

A theory for determining the rate of nuclei formation is advanced by Volmer (reference 2). It is assumed that aggregates of the size defined by equation (1) are the condensation nuclei of the supersonic stream. Volmer's equation is modified in appendix A to the following more convenient expression:

$$\log_e J = \log_e 9.589 \times 10^{25} + \log_e \left[\left(\frac{p_\infty}{t} \right)^2 K_E^{1/2} \frac{m^{1/6}}{\rho_l^{2/3}} \right] + 2 \log_e p_v/p_\infty - 17.558 \left(\frac{K_E}{t} \right)^3 (\log_e p_v/p_\infty)^{-2} \quad (2)$$

where

J rate of formation of nuclei, number per second per cubic centimeter

K_E $S \left(\frac{m}{\rho_l} \right)^{2/3}$, ergs

(All symbols used herein are defined in appendix A.)

The estimated variation of K_E with temperature is discussed in appendix B and presented in figure 1. The saturation-vapor pressures p_∞ for supercooled water were determined from a relation

by Osborne and Meyers (see reference 5). The density of water, used to the 2/3 power in the second term of the right side of equation (2), was obtained by extrapolation of the measured values given in reference 6. Because of the slight change in density with temperature, the effect of any error in the density (used to the 2/3 power) on the value of $\log_e J$ was considered negligible. The variation of $\log_e J$ of equation (2) with vapor-pressure ratio (expressed as $\log_e p_v/p_\infty$) for selected isotherms is presented in figure 2. The sensitivity of the nuclei formation rate to the vapor-pressure ratio is characterized by the steep slopes of the isotherms (fig. 2); for example, for a gas temperature of -54.4° F, a change in nuclei formation rate from 1 to 20,000 per second per cubic centimeter corresponded to a change in vapor-pressure ratio from 10.3 to 13.2

In order to associate the relation of figure 2 with the properties of a gas flowing through a supersonic tunnel, curves AB and BC are presented. If the temperature of the air entering a supersonic tunnel is increased, the vapor pressures p_v in the tunnel remain constant but the saturation-vapor pressures p_∞ change. The resulting relation between local stream temperature t and the quantity $\log_e (p_v/p_\infty)$ at a given local Mach number is illustrated by curve AB (directed from A to B). The rate of nuclei formation at the station, and hence the tendency for condensation, is decreased. If, having reached the conditions corresponding to B for the given station, the humidity and the temperature of the inlet air are maintained constant and flow conditions at higher Mach numbers farther along the tunnel are considered, the curve BC is indicative of the accompanying trend in the tendency for condensation, the value of J increasing with an increase in Mach number. Thus, if the value of J required for condensation is attained in the tunnel, increasing the temperature lowers the J value at each station and expansion to a higher Mach number is required before the critical J is again reached. The experimental problem is to determine J for condensation-free flow. The experimental data in figure 2 are presented later.

APPARATUS

The tunnel system (fig. 3) is a nonreturn steady-flow type. The specific humidity of the inlet air can be varied from a minimum specific humidity of 0.00025 pound per pound of dry air to a specific

humidity corresponding to saturation. The inlet-air dew points (hereinafter called dew points) were determined to within ±0.5° F by simultaneous use of a continuously indicating electronic dew-point meter (reference 7), a manually operated dew-point meter, and an expansion-type dew-point meter. The inlet-air stagnation temperature (hereinafter called inlet temperature) can be regulated from 40° to 250° F by means of thermostatic controls and was measured with a 5/16-inch aspirating thermocouple (reference 8) and a self-balancing potentiometer to within ±0.5° F.

Tunnels with 3.4- by 3.4-inch and 4- by 10-inch test sections were used in the investigations. Three interchangeable nozzles were available for the 3.4- by 3.4-inch tunnel. One nozzle was designed for a Mach number of 2.00 with a straight diverging wall (included angle of 3.50°). The throat was faired into the plane diverging-wall section by use of an arbitrary radius. This nozzle installation is shown in figure 4(a). The other two nozzles were designed by the source-flow method (reference 9) for Mach numbers of 2.01 and 1.45 (figs. 4(b) and 4(c), respectively). The nozzle used in the 4- by 10-inch tunnel was also designed by the source-flow method for a Mach number of 2.00 (fig. 4(d)). An approximate correction for viscosity effects was made in the design of the source-flow nozzles in order to attain the design Mach number in practice.

Each tunnel was equipped with wall orifices of approximately 0.013-inch diameter throughout the expanding surfaces and side plates. Typical side-plate instrumentation is presented in figure 4(e). The orifices, as well as the pitot rakes located at the inlet and the outlet of each tunnel, were coupled with multiple-tube mercury manometers that could be simultaneously photographed. The change in height of any mercury column could be read to the nearest 0.005 inch by means of special viewers. The orifices of the 4- by 10-inch tunnel could also be coupled with a multiple-tube oil manometer, on which a change in column height corresponding to 0.0006 inch of mercury could be detected.

RESULTS AND DISCUSSION

Condensation-Free Criterions

The increase in static pressure of a supersonic stream passing through a condensation shock is theoretically predicted in appendix C and is experimentally established in reference 1. This increase in static pressure can be used to determine the location

of a condensation shock in a supersonic tunnel. An example of the experimental data used in determining the shock location is shown in figure 5. The variation in static-pressure ratio p/P_0 with inlet temperature T_0 at one arbitrary station in a supersonic nozzle is presented for a dew point of 56° F. (Dew point is defined as the temperature at which the liquid, or solid, and vapor phases coexist for a given partial pressure of the vapor. Temperatures for the remainder of the report will be given in English units.) The shock was moved along the nozzle in the direction of increasing Mach number by raising the inlet temperature. At an inlet temperature of 160° F (point A in fig. 5), a minimum static-pressure ratio of 0.201 was reached and all measurable effects of the condensation shock were downstream of the station. An inlet temperature of 160° F is the minimum required for condensation-free flow at the given station and dew point and is designated the critical temperature T_c.

If the critical temperature corresponding to each station throughout the supersonic nozzle and the test section of a tunnel is established, the position of the condensation shock as a function of the inlet temperature is determined. Critical temperatures were obtained at stations throughout the nozzles of the 3.4- by 3.4-inch tunnel by varying the inlet temperature and maintaining the dew point constant at 18° to 23.5°, 49°, and 56° ±1° F (table I, investigations 1, 2, and 3, respectively). These critical temperatures are presented in figure 6 as a function of the experimental Mach numbers measured at the tunnel stations. The conditions required for condensation-free flow at a given dew point must fall below the curve corresponding to the dew point. The shock movement throughout the test section of the tunnel of 1.45 Mach number (3.4- by 3.4-in. test section) is presented in figure 7 in a manner similar to that for the nozzles of figure 6 for dew points of 10.8°, 20.0°, 26.8°, and 44.5° F (table I, investigations 4, 5, 6, and 7, respectively). In recording the movement of the shock through the test section, however, the location of each station (referenced from the test-section inlet) is used (fig. 7) in place of Mach number because the Mach number throughout the test section is nearly constant. The shock was moved down the nozzle (in the direction of increasing Mach number) and through a considerable part of the constant-area test section by increasing the inlet temperature. An inlet temperature was ultimately attained at which the shock appeared to move suddenly out of the test section; that is, the critical temperatures for the stations downstream of the last observed shock position were reached simultaneously. This inlet temperature T_s (fig. 7) corresponds to the data that appear to approach vertical lines.

The stream temperature and the vapor-pressure ratio and thus the nuclei formation rate corresponding to condensation-free flow in the test section of the 3.4- by 3.4-inch tunnel were established for each inlet stagnation temperature T_s of figure 7 and are presented in figure 2. The stream temperature was obtained from T_s and the energy relation

$$\frac{t}{T_s} = \left(1 + \frac{\gamma - 1}{2} M^2\right)^{-1} \tag{3}$$

where M is the Mach number at the test-section inlet. The vapor pressure of water p_∞ at the stream temperature was calculated by means of reference 5. The partial pressure of the vapor p_v at the test-section inlet was determined by using a combination of Dalton's law of partial pressures and the perfect gas law. The specific humidity σ in pounds of water vapor per pound of dry air is therefore

$$\sigma = 0.6223 \frac{p_v}{p - p_v} \tag{4}$$

Measured values of inlet pressure and dew point were used to obtain the inlet specific humidity. Any change in the specific humidity prior to the condensation shock was considered negligible. The stream pressure p was measured with wall orifices.

The experimental procedure used in investigations 4 to 7 (table I) in the 3.4- by 3.4-inch tunnel was also used for investigations 8 and 9, which were made at a Mach number of 2.00 in the 4- by 10-inch tunnel.

The critical temperatures throughout the constant-area test section are presented in figure 8. The curves in figure 8 do not appear to approach vertical asymptotes as do those of figure 7, but are inclined with a positive and nearly constant slope. This positive slope is more in keeping with the nuclei theory of condensation than is the infinite slope of figure 7, because as the stream temperature increases and the rate of formation of condensation nuclei decreases it is reasonable to believe that a greater time (and thus a greater distance) would be required for the completion of the condensation process. An explanation of the apparently infinite slope of figure 7 may be that the slope of test-section distance for a given change in inlet temperature at the high dew points of investigations 4 to 7 is too great to be

detected in a tunnel having the limited length of the 3.4- by 3.4-inch tunnel. Also, the boundary-layer growth, known to have a greater effect on the flow properties in small tunnels than in large tunnels, may have restrained the condensation in the test section through an increase in the saturation pressure of the vapor accompanying the deceleration of the flow.

If the first 14 inches of test section of the 4- by 10-inch tunnel is considered to be the test section, and the nuclei formation rates corresponding to the critical temperatures at 14 inches from the test-section inlet (fig. 8) are calculated in the same way as was done for the inlet temperature T_s in the 3.4- by 3.4-inch tunnel, the average nuclei formation rate compares well with the average rate required for condensation-free flow in the 3.4- by 3.4-inch tunnel (fig. 2).

A condensation-free-criterions chart based on the Volmer theory for nuclei formation may be constructed from figure 2. The chart will apply to tunnels comparable in size to the 3.4- by 3.4-inch tunnel and also to tunnels comparable in size to the 4- by 10-inch tunnel and having test sections approximately 14 inches in length. The average of the six experimentally determined values of $\log_e J$ (fig. 2) was selected as the criterion for condensation-free flow and designated $\log_e J_c$. The variation of stream temperature with vapor-pressure ratio required for condensation-free flow (fig. 9) corresponding to this criterion was obtained from a cross plot of figure 2 at $\log_e J = \log_e J_c$.

The relation between the properties of the tunnel air and the criterion may be illustrated with the curve AB of figure 2, as presented in figure 9. If the gas temperature at a station in the tunnel is increased (moving from A to B), the corresponding decrease in the degree of saturation is such that the curve passes to the left of the criterion curve into the region of condensation-free flow.

The relation given in figure 9 may be expressed in terms of the more convenient tunnel operating parameters of temperature, Mach number, and dew point. Calculations were made for various values of stream temperature t and inlet temperature T. The Mach number corresponding to any selected t/T was calculated using equation (3). For a given value of t, $\log_e (p_v/p_\infty)$ was obtained from figure 9 and the saturation-vapor pressure p_∞ was evaluated in accordance with the Osborne-Meyer relation (reference 5). Hence

the partial pressure of the vapor p_v was determined. The assumption, justifiable in most cases, is made that p_v and P_v are negligible compared with p and P, respectively, and that σ is constant. It follows from equation (4) that $p_v/P_v = p/P$ and thus the partial pressure of the vapor at stagnation may be calculated from the isentropic relation

$$\frac{p_v}{P_v} = \left(1 + \frac{\gamma - 1}{2} M^2\right)^{-\frac{\gamma}{\gamma-1}} \qquad (5)$$

A condensation-free-criterions chart relating the partial pressure of the vapor at the tunnel inlet (expressed as dew point), the inlet temperature, and the test-section Mach number for the tunnels used in the investigation reported is presented in figure 10. The inlet temperatures are indicated with solid lines and the stream temperatures used in the calculation are shown as dashed lines. Although the properties of supercooled water were used in the calculations, frost-point rather than dew-point temperatures were used on the chart below 32° F, because the usual dew-point meters read frost point in this range.

The results of the experimental investigations used in determining $\log_e J_c$ are also presented in figure 10. The numbers by the symbols indicate the measured inlet stagnation temperature. The deviation of the experimental values of $\log_e J$ from $\log_e J_c$ in figure 2 correspond in figure 10 to dew-point fluctuations of approximately ±1.5° F or to inlet-temperature changes of approximately ±2° F.

No assumption was made regarding tunnel-inlet pressure in the calculation of figure 10, except that the dew point be measured at the tunnel-inlet pressure. The partial pressure of the vapor (expressed as dew point), the specific humidity, and the mixture pressure (water-vapor pressure plus air pressure) are presented in convenient form in figure 11 in accordance with equation (4). Frost points rather than dew points were again used below 32° F. Figure 11 combined with the condensation-free-criterions chart (fig. 10) can be used to predict the tunnel-inlet-air properties required for condensation-free flow in the tunnel test section for tunnels comparable in size with the 3.4- by 3.4-inch and 4- by 10-inch tunnels and operating over a range of inlet pressures. For example, consider a tunnel operating with an inlet pressure of 100 pounds per square inch absolute and having a test-section

Mach number of 2.00. Assume that, because of the available drying apparatus, the minimum specific humidity of the air at 100 pounds per square inch absolute is 0.0002 pound per pound of dry air. From figure 11, a specific humidity of 0.0002 corresponds to a dew point of 10.5° F at an inlet pressure of 100 pounds per square inch absolute. From figure 10, the inlet stagnation temperature (solid lines) corresponding to a Mach number of 2.00 and a dew point of 10.5° F is approximately 228° F. This temperature corresponds to the minimum value required for condensation-free flow in the tunnel test section. In practice, it would be advisable to exceed the minimum temperature as a protection against the possibility of local regions of higher Mach number "triggering" the condensation process.

The condensation-free criterions of figure 10 were based on investigations made at a Mach number of 1.45 in a 3.4- by 3.4-inch tunnel and at a Mach number of 2.00 in a 4- by 10-inch tunnel with a 14-inch test section. An additional investigation (10, table I) at Mach number 2.01 and dew point 17.3° F was made in the 3.4- by 3.4-inch tunnel to ascertain the effect of tunnel Mach number on the conditions necessary for condensation-free flow. An inlet-stagnation temperature of 246° F was required for condensation-free flow throughout the test section as compared with the inlet stagnation temperature predicted in figure 10 of 243° F. Although one investigation may not be considered conclusive, it does indicate that theoretical extension of the data for a Mach number of 1.45 on a basis of nuclei-formation theory is valid up to a Mach number of 2.01. Preliminary unpublished data of tunnels operated at several Mach numbers up to and including a Mach number of 2.00 and having sizes $1\frac{1}{2}$ to 2 times that of the 4- by 10-inch tunnel, substantiate (±10° F inlet stagnation temperature for a given dew point and Mach number) the chart of figure 10.

Scale Effect

The extension of figure 10 to tunnels having test sections of considerable length, however, requires further consideration because of the scale effect apparent in figure 8. It was found that an increase in test-section length necessitated an increase in inlet temperature to avoid condensation. The increase in inlet temperature per foot increase in test-section length for the 4- by 10-inch tunnel (Mach number of 2.00) was 5.3° and 6° F for inlet dew points of -5° and -10° F, respectively. This observed scale effect agrees with preliminary unpublished NACA data for a tunnel 5 times the size of the 4- by 10-inch tunnel.

A scale effect was also noticed in the difference between the movement of the shock through the nozzles of 2.01 Mach number of the 3.4- by 3.4-inch tunnel (dew point 17.3° F) and 2.00 Mach number of the 4- by 10-inch tunnel (dew point 19° F), which may be attributed to the different rates of expansion of the flow in the two nozzles and the time required for the condensation process. For a given temperature (fig. 12), the shock occurred at a higher Mach number in the nozzle of the 3.4- by 3.4-inch tunnel than in the nozzle of the 4- by 10-inch tunnel, the 3.4- by 3.4-inch tunnel nozzle expanding the flow to a Mach number of 2.00 in less than one-third the distance required by the 4- by 10-inch tunnel nozzle. Hence the data obtained throughout the nozzles are not generally acceptable for use in constructing criterion charts.

The criterion $\log_e J_c$ was determined using vapor pressures over supercooled water rather than over ice, even though the stream temperatures in the region of the condensation shock were well below freezing. Although no conclusive evidence regarding the physical state of the condensation droplets has yet been obtained, it has been observed that ice formations on tunnel walls and models occur only under conditions of extreme moisture content and recovery temperatures close to freezing. An ice formation on the glass sides of the 3.4- by 3.4-inch tunnel (nozzle Mach number, 1.45) is shown in figure 13 for a dew point of approximately 70° F and an inlet temperature such that, with 90-percent recovery of the kinetic energy, the wall temperature was a few degrees above freezing.

Physical Appearance of Condensation Shock

Schlieren photographs of condensation shocks are presented in figure 14. Figures 14(a) and 14(b) are photographs of a shock located in a channel having no curvature just downstream of the throat, and figures 14(c) and 14(d) are photographs of a shock in a nozzle having considerable curvature from the region of the throat to the test section. In figure 14(a) the shock, located just downstream of the throat, appeared well defined and extended over a relatively small distance; whereas in figure 14(b) the shock, having been moved into a region of higher velocity, appeared poorly defined and extended over a considerably greater distance in the direction of the flow. The shock in both positions appeared to be normal to the stream. In the nozzle having considerable curvature, the shock located just downstream of the throat was also normal to the stream and well defined, as presented in figure 14(c). As the shock was moved downstream, it again required a greater distance to attain completion (fig. 14(d)) and at the same time was changed

from a shock normal to the stream to one having an X-shape. In figure 14(d), well-defined disturbances appeared to be passed back and forth across the tunnel downstream of the shock.

Practical Considerations for Tunnel Design

The obvious way to insure flow that is free from condensation effects is to eliminate the condensation shock by drying or heating the air or both in accordance with criterions such as those presented in figure 10. The requirements, however, become rapidly prohibitive as the tunnel Mach number increases. Specifications must therefore be established for the maximum allowable vapor content of the inlet air at and below which condensation effects are negligible. No attempt has been made to determine precisely such criterions. Information was gathered during the investigations discussed herein, however, that may be used for a qualitative approach to the problem. The magnitude of the change in static pressure along the walls of the test-section inlets was observed for several specific humidities at Mach numbers of 1.45 and 2.01 in the 3.4- by 3.4-inch tunnel and at a Mach number of 2.00 in the 4- by 10-inch tunnel. The change in static pressure across the shock for the two Mach numbers is presented in figure 15 as a function of the specific humidity. The difference between the average pressure ratio behind the shock (pressure ratio at B in fig. 5) and the pressure ratio corresponding to the minimum pressure ahead of the shock (pressure ratio at A in fig. 5) for stations at the test-section inlet was averaged to arrive at the change in static-pressure ratio $\frac{p_2 - p_1}{p_0}$ of figure 15. The theoretical $\frac{p_2 - p_1}{p_0}$ was calculated for Mach numbers of 1.45 and 2.00 as a function of specific humidity in accordance with appendix B. It appears from experiment and theory that for a given Mach number, $\frac{p_2 - p_1}{p_0}$ increases with an increase in specific humidity and that the magnitude of $\frac{p_2 - p_1}{p_0}$ for a given specific humidity decreases with an increase in test-section Mach number.

SUMMARY OF RESULTS

From an experimental investigation of condensation shock in supersonic tunnels, the following results were obtained:

1. The Volmer theory of nuclei formation and an experimental determination of the rate of formation of nuclei required for a condensation shock were combined to establish criterions for condensation-free flow in a 3.4- by 3.4-inch tunnel and a 4- by 10-inch tunnel with a 14-inch test section.

2. An increase in inlet temperature was required to avoid condensation when the test section of the 4- by 10-inch tunnel was lengthened, inlet dew point and Mach number remaining constant. This scale effect was found to agree with unpublished NACA data for a tunnel five times the size of the 4- by 10-inch tunnel.

3. The static-pressure rise across a condensation shock located in the test-section inlet of a tunnel increased with an increase in specific humidity for a given test-section Mach number, and, for a given specific humidity, decreased with an increase in Mach number, as predicted by theory.

Lewis Flight Propulsion Laboratory
National Advisory Committee for Aeronautics
Cleveland, Ohio, June 16, 1949

APPENDIX A

SYMBOLS

The following symbols are used in this report:

C_p	specific heat at constant pressure
C_v	specific heat at constant volume
J	rate of formation of nuclei, number/(sec)(cc)
K_E	$S\left(\frac{m}{\rho_l}\right)^{2/3}$, ergs
M	Mach number
m	molecular weight of vapor, gram/mole
P	stagnation pressure
P_v	partial pressure of vapor at stagnation
p	static pressure
p_v	partial pressure of vapor
p_∞	saturation-vapor pressure in equilibrium with infinite liquid surface, mm Hg
p_v/p_∞	ratio of partial pressure of vapor to saturation-vapor pressure (relative humidity)
q	heat added to flow at condensation shock, ft-lb/lb dry air
R	universal gas constant, joules/($^\circ$C)(mole)
r	radius of aggregate, cm
S	surface tension of liquid, dynes/cm
T	inlet-air stagnation temperature
T_c	critical temperature (inlet-air stagnation temperature corresponding to condensation-free flow at a given station)

T_s inlet-air stagnation temperature corresponding to condensation-free flow in tunnel test section

t stream temperature

V velocity, ft/sec

γ ratio of specific heats, C_p/C_v

ρ density, grams/cc

ρ_l density of liquid, grams/cc

σ specific humidity, lb water vapor/lb dry air

τ duration of state of greatest supersaturation, sec

Subscripts:

0 before tunnel inlet

1 before condensation shock

2 after condensation shock

APPENDIX B

MODIFICATION OF VOLMER THEORY

A theory for determining the rate of nuclei formation is presented by Volmer in reference 2. The probability of the formation of nuclei is evaluated therein (p. 136) as

$$\log_e J\tau = \log_e \tau + \log_e (9.5 \times 10^{25}) + \log_e \left[\left(\frac{p_\infty}{t} \right)^2 \frac{\sqrt{Sm}}{\rho_l} \right] + 2 \log_e \frac{p_v}{p_\infty} - 17.49 \left(\frac{m}{\rho_l} \right)^2 \left(\frac{S}{t} \right)^3 \left(\frac{1}{\log_e \frac{p_v}{p_\infty}} \right)^2 \qquad (B1)$$

where

9.5×10^{25} combination of physical constants, $\left[\frac{\text{deg}}{(\text{dyne})(\text{cm})} \right]^2$

17.49 combination of physical constants, $\frac{(\text{mole}^2)(\text{deg}^3)}{(\text{dyne}^3)(\text{cc})}$

The combinations of the physical constants were corrected herein to agree with the currently accepted values of the universal gas constant and Boltzmann's constant. Accordingly, 9.5×10^{25} was changed to 9.589×10^{25} and 17.49 was changed to 17.558.

During the expansion of the air through the tunnel and the accompanying change in stream temperature and vapor-pressure ratio, the only significant change in the value of the terms on the right side of equation (B1) occurs in the last term, now corrected to

$$17.558 \left(\frac{m}{\rho_l} \right)^2 \left(\frac{S}{t} \right)^3 \left(\frac{1}{\log_e \frac{p_v}{p_\infty}} \right)^2$$

The inherent difficulty in applying the Volmer theory is apparent upon examination of this term when it is realized that the correct values of surface tension and density of water must be determined for stream temperatures well below freezing. It is proposed that surface tension, density, and molecular weight be combined as

$$K_E = S\left(\frac{m}{\rho_l}\right)^{2/3}$$

for purposes of extrapolating their known values, inasmuch as the rate of change of K_E with temperature is nearly constant over the known range. A plot of K_E calculated from the physical properties of water in accordance with reference 6 is presented in figure 1. Because of the difficulty of measuring the properties of supercooled water (the admitted possibility for error is shown by the shaded area), the experimental upward trend of K_E below 273° K was neglected and the data above the freezing point were extrapolated linearly to 170° K. If K_E is introduced into equation (B1), and the duration of critical conditions $\log_e \tau$ is dropped from both sides of equation (B1), the equation may be written

$$\log_e J = \log_e 9.589 \times 10^{25} + \log_e \left[\left(\frac{p_\infty}{t}\right)^2 K_E{}^{1/2} \frac{m^{1/6}}{\rho_l{}^{2/3}}\right] + 2 \log_e \frac{p_v}{p_\infty} - 17.558 \left(\frac{K_E}{t}\right)^3 \left(\log_e \frac{p_v}{p_\infty}\right)^{-2} \qquad (B2)$$

APPENDIX C

CHANGE IN STATE ACROSS CONDENSATION SHOCK

The usual flow relations may be used to obtain a one-dimensional approximation of the change in state across a condensation shock. The following assumptions greatly simplify the calculations (see following figure):

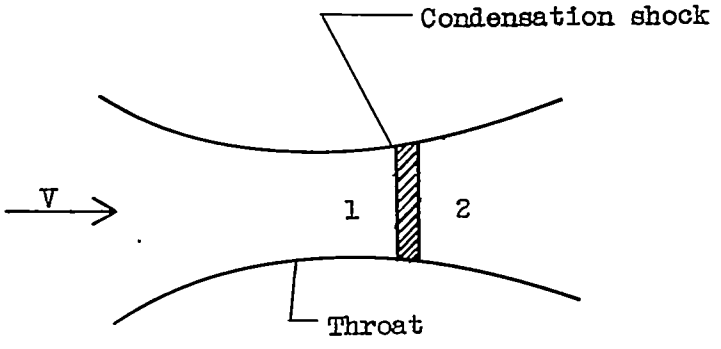

The shock takes place at constant area, the specific heats before and after condensation do not change, the gas constant of the air is not appreciably affected by the moisture of the air, and all the moisture condenses out at the shock until saturation is reached. The energy relation may be written

$$C_p t_1 + \frac{V_1^2}{2} + q = C_p t_2 + \frac{V_2^2}{2} \tag{C1}$$

Relation (C1) may be rearranged into the form

$$\frac{t_2}{t_1} = \frac{\frac{q}{\gamma R t_1} + \frac{1}{\gamma - 1} + \frac{M_1^2}{2}}{\frac{1}{\gamma - 1} + \frac{M_2^2}{2}} \tag{C2}$$

With the momentum relation,

$$p_1 + \rho_1 V_1^2 = p_2 + \rho_2 V_2^2 \tag{C3}$$

and the perfect gas law,

$$p = \rho R t \tag{C4}$$

and the assumption of conservation of mass, relation (C2) may be rearranged to give

$$\frac{\frac{1}{\gamma - 1} + \frac{M_2^2}{2}}{\left(\frac{1 + \gamma M_2^2}{M_2}\right)^2} = \frac{\frac{q}{\gamma R t_1} + \frac{1}{\gamma - 1} + \frac{M_1^2}{2}}{\left(\frac{1 + \gamma M_1^2}{M_1}\right)^2} \tag{C5}$$

The value of M_1 may be determined from the criterions chart (fig. 10) if the specific humidity and the inlet temperature are known. The correct value of q is obtained by a series of approximations (temperature and q are interdependent). Hence M_2 is determined. The effect of the condensation shock upon the stream pressure may then be determined from equation (C3), rearranged to give

$$\frac{p_2}{p_1} = \frac{1 + \gamma M_1^2}{1 + \gamma M_2^2} \tag{C6}$$

Equation (C6) and the isentropic relation

$$\frac{p_1}{P_1} = \left(1 + \frac{\gamma - 1}{2} M^2\right)^{-\frac{\gamma}{\gamma - 1}} \tag{C7}$$

may be used to calculate the change in static pressure as presented in figure 15.

REFERENCES

1. Hermann, R.: Condensation Shock Waves in Supersonic Wind Tunnel Nozzles. British R.T.P. Trans. No. 1581, M.A.P.

2. Volmer, Max.: Kinetik Der Phasenbildung. Chemische Reaktion, Bd. IV. K. F. Bonhoeffer (Dresden und Leipzig), 1939.

3. Oswatitsch, Kl.: Condensation Phenomena in Supersonic Nozzles. British R.T.P. Trans. No. 1905, M.A.P.

4. Das Gupta, N. N., and Ghosh, S. K.: A Report on the Wilson Cloud Chamber and Its Applications in Physics. Rev. Modern Phys., vol. 18, no. 2, April 1946, pp. 225-290.

5. Dorsey, N. Ernest: Properties of Ordinary Water-Substance. Reinhold Pub. Corp. (New York), 1940, p. 574.

6. Anon.: International Critical Tables. Vol. VII. McGraw-Hill Book Co., Inc., 1930.

7. Friswold, Frank A., Lewis, Ralph D., and Wheeler, R. Clyde, Jr.: An Improved Continuous-Indicating Dew-Point Meter. NACA TN 1215, 1947.

8. Lindsey, W. F.: Calibration of Three Temperature Probes and a Pressure Probe at High Speeds. NACA ARR, April 1942.

9. Foelsch, Kuno: A New Method of Designing Two-Dimensional Laval Nozzles for a Parallel and Uniform Jet. Rep. No. NA-46-235-2, Thermodynamics Sec., Eng. Dept., North American Aviation, Inc., May 27, 1946.

10. Anon.: Heating, Ventilating, Air Conditioning Guide. Vol. 25. Pub. by Am. Soc. Heating and Ventilating Eng. (New York), 1947, pp. 26-36.

TABLE I - INVESTIGATIONS OF CONDENSATION IN SUPERSONIC FLOW

Investigation	Test-section Mach number	Dew point (°F)	Tunnel (in.)
1	No test section	18-23.5	3.4 by 3.4
2	2.01	49	3.4 by 3.4
3	No test section	56±1	3.4 by 3.4
4	1.45	10.8	3.4 by 3.4
5	1.45	20.0	3.4 by 3.4
6	1.45	26.8	3.4 by 3.4
7	1.45	44.5	3.4 by 3.4
8	2.00	-5	4 by 10
9	2.00	-10	4 by 10
10	2.01	17.3	3.4 by 3.4
11	2.00	19	4 by 10

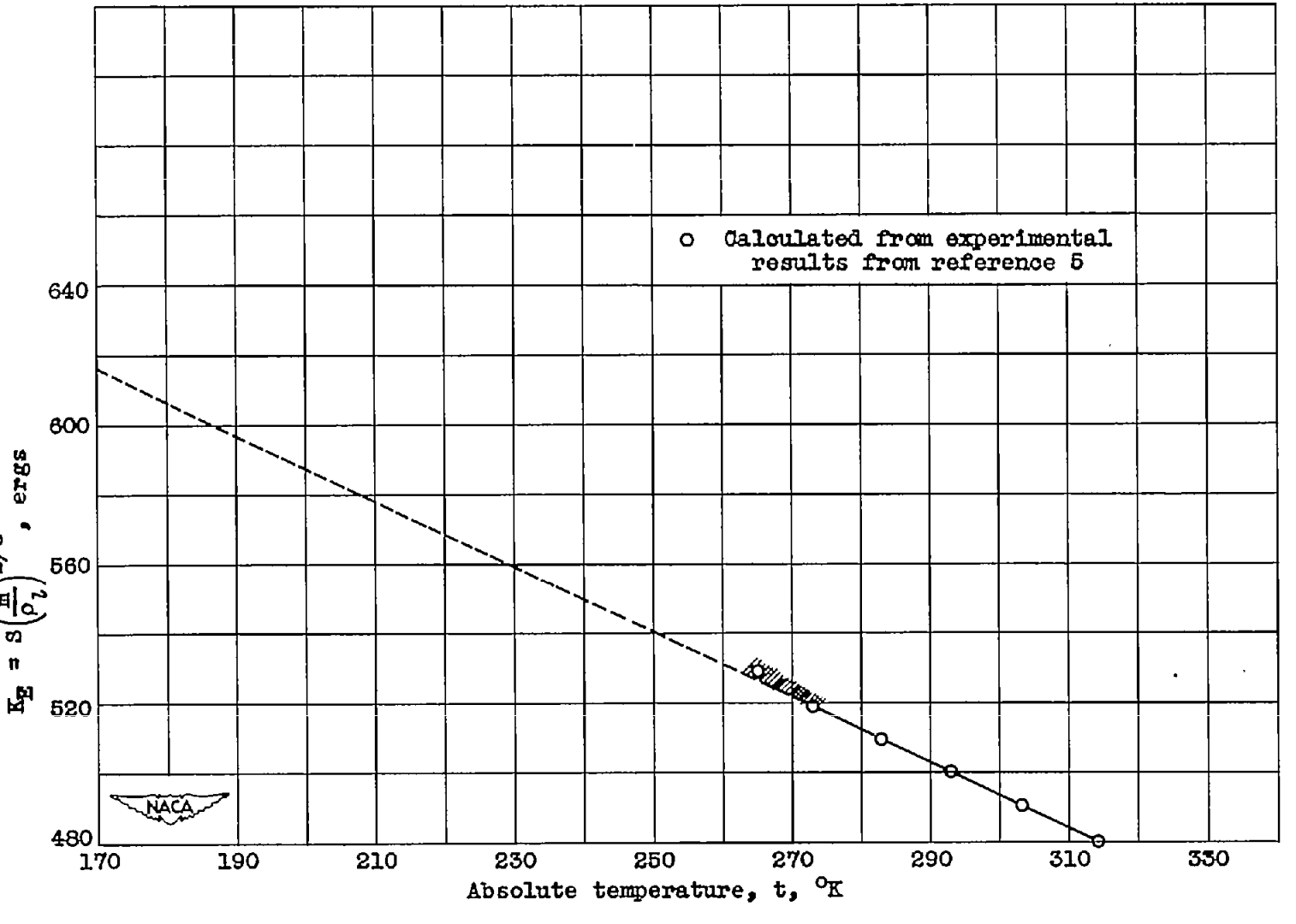

Figure 1. - Variation of K_E with temperature.

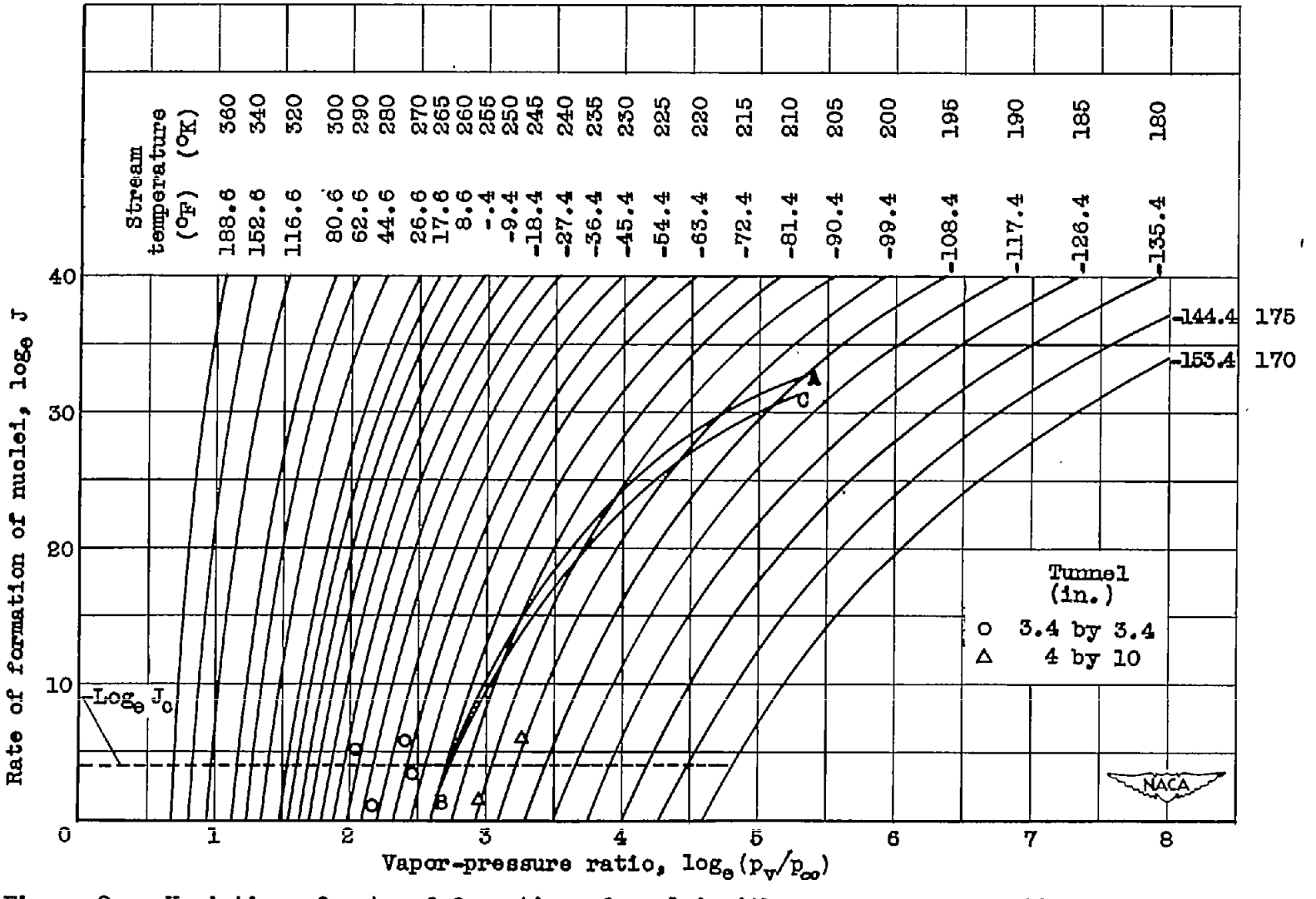

Figure 2. - Variation of rate of formation of nuclei with vapor-pressure ratio for various isotherms.

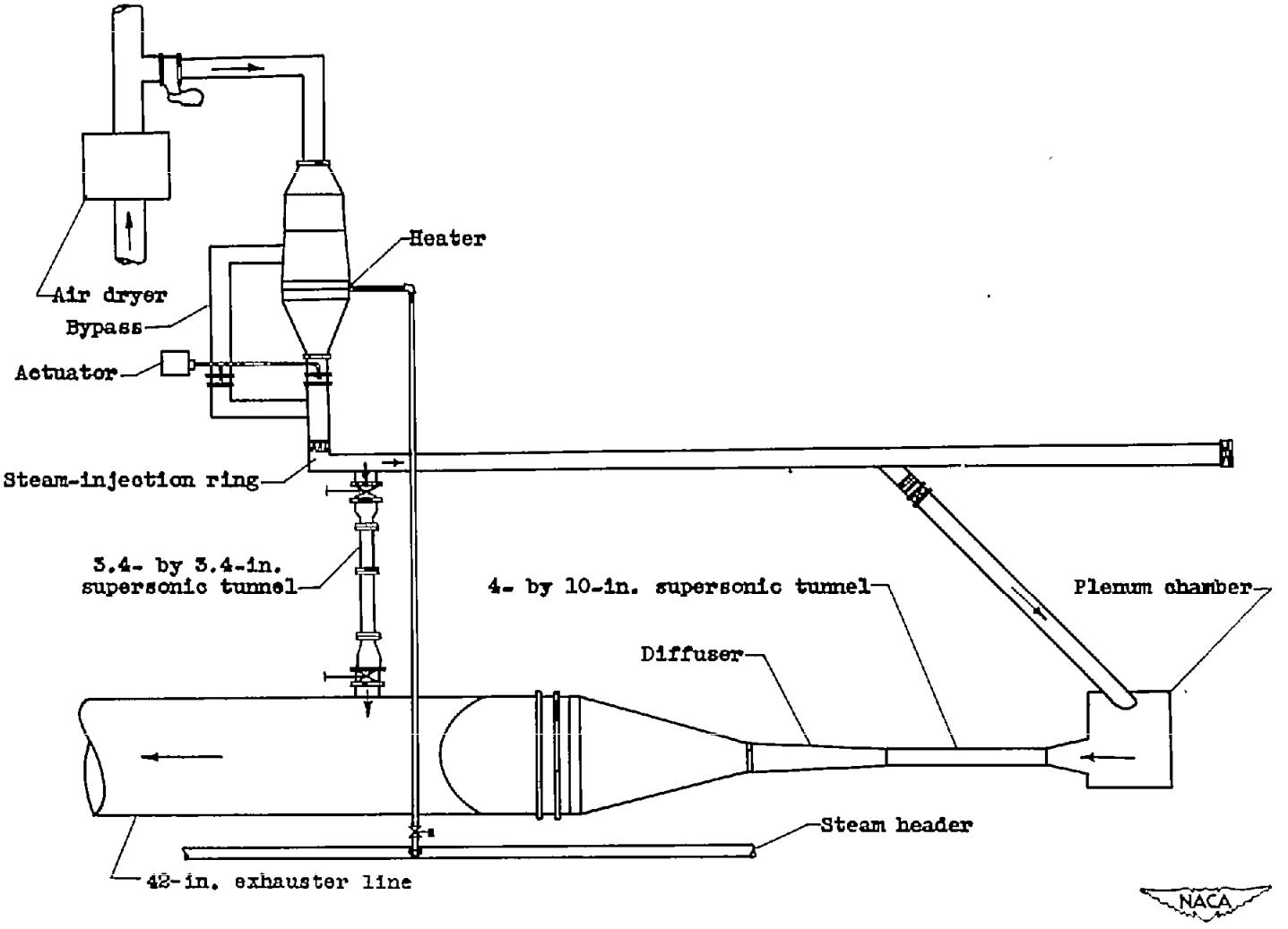

Figure 3. - Diagrammatic sketch of tunnel system.

(a) 3.4- by 3.4-inch tunnel nozzle installation with included angle of 3.50°; nozzle in place; Mach number, 2.00.

NACA C-21254 4-21-48

(b) 3.4- by 3.4-inch tunnel nozzle; Mach number, 2.01.

NACA C-21284 4-21-48

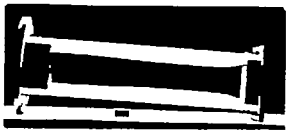

(c) 3.4- by 3.4-inch tunnel nozzle; Mach number, 1.45.

NACA C-21288 4-21-46

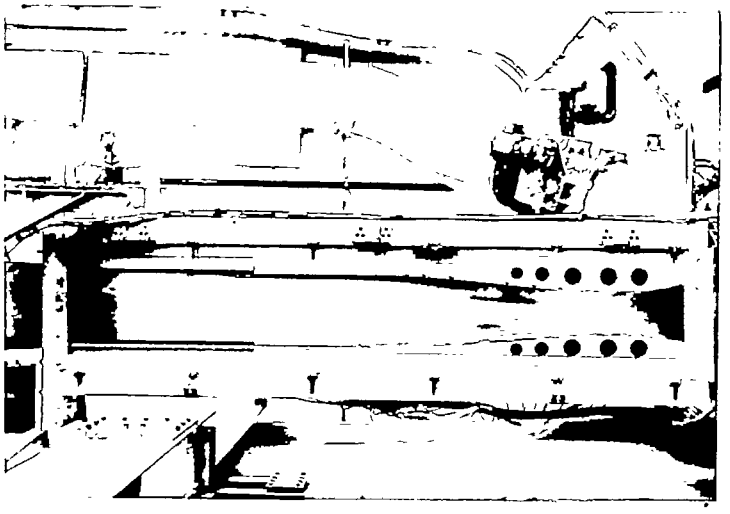

(d) 4- by 10-inch tunnel installation showing nozzle; Mach number, 2.00.

NACA C-21290 4-21-48

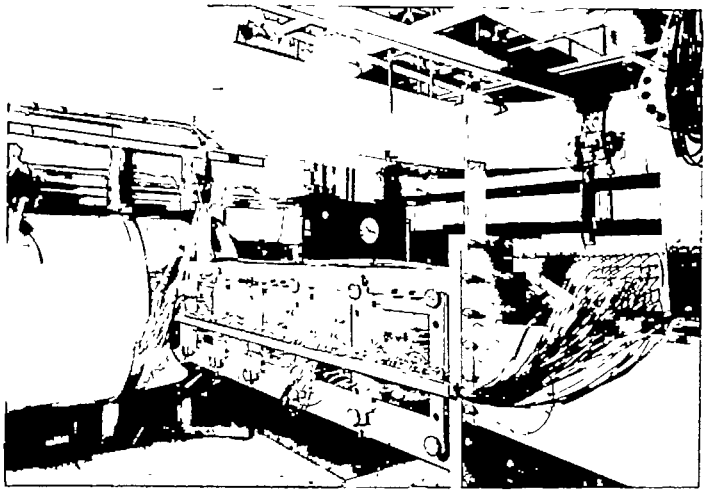

(e) 4- by 10-inch tunnel installation showing instrumentation.

NACA C-21291 4-21-48

Figure 4. - Installations and nozzles of 3.4- by 3.4-inch and 4- by 10-inch tunnels.

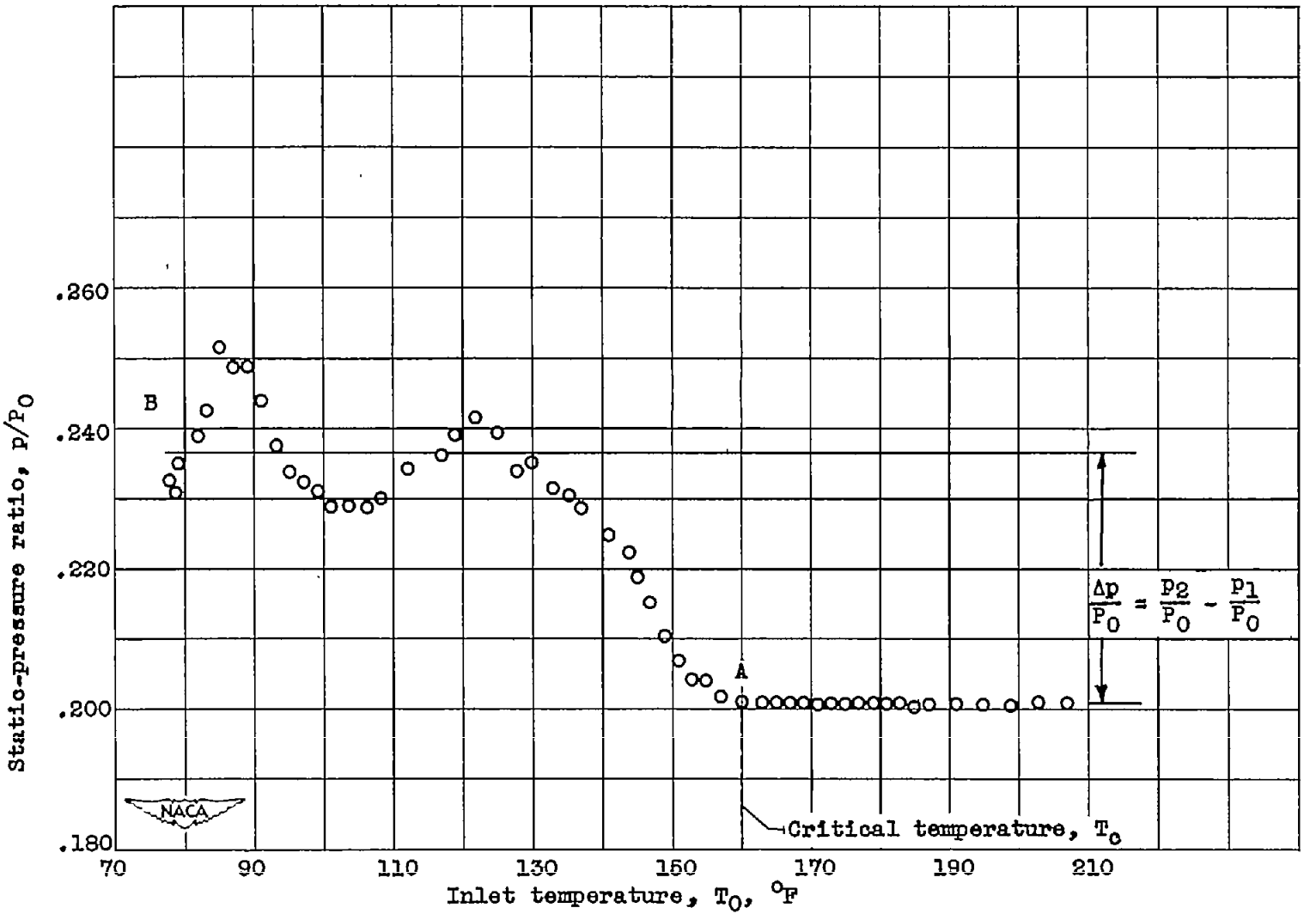

Figure 5. - Variation of static-pressure ratio with inlet temperature for given station. Dew point, 56° F.

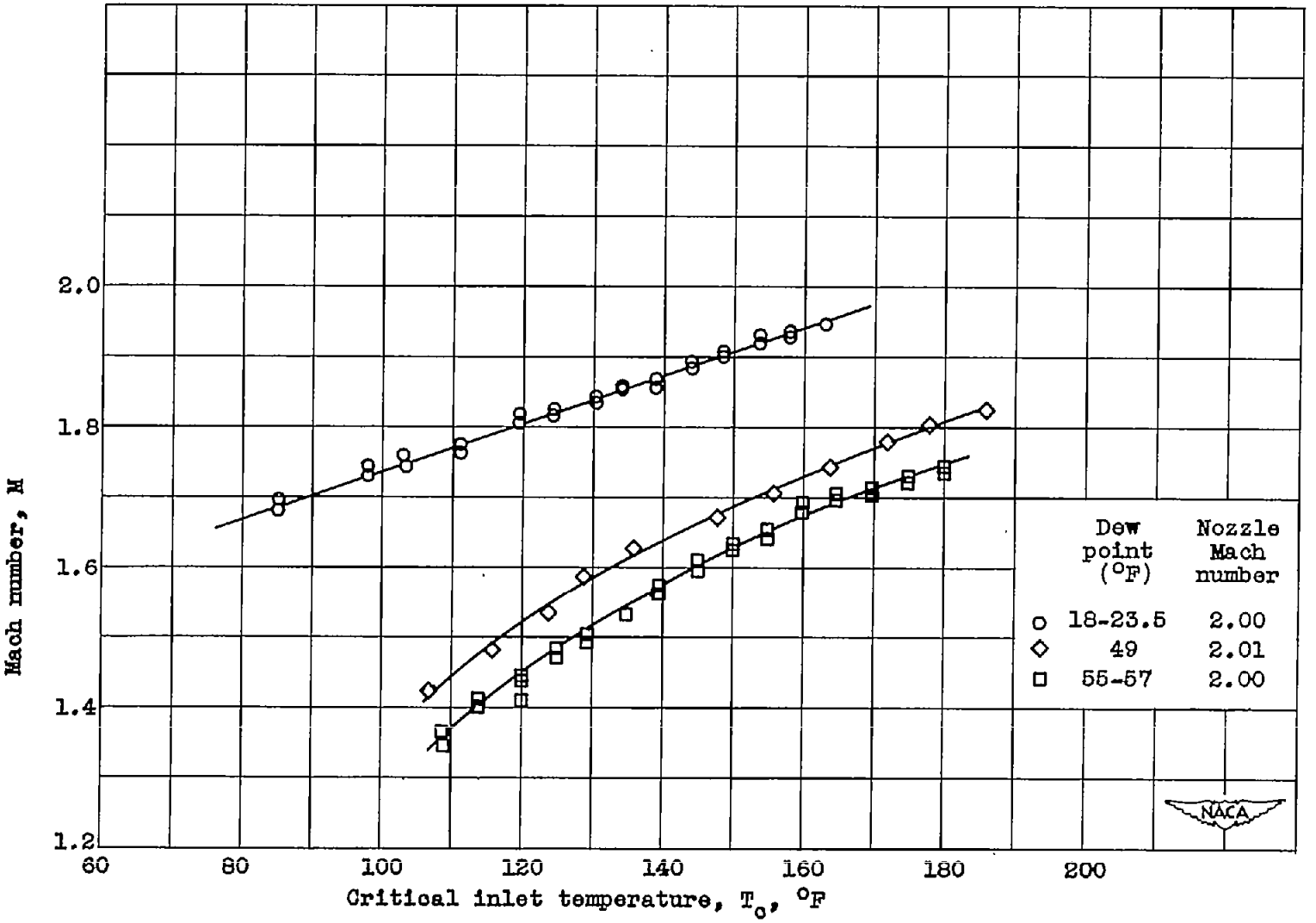

Figure 6. - Relation between Mach number and critical temperatures throughout nozzles of 3.4- by 3.4-inch tunnel at three dew points.

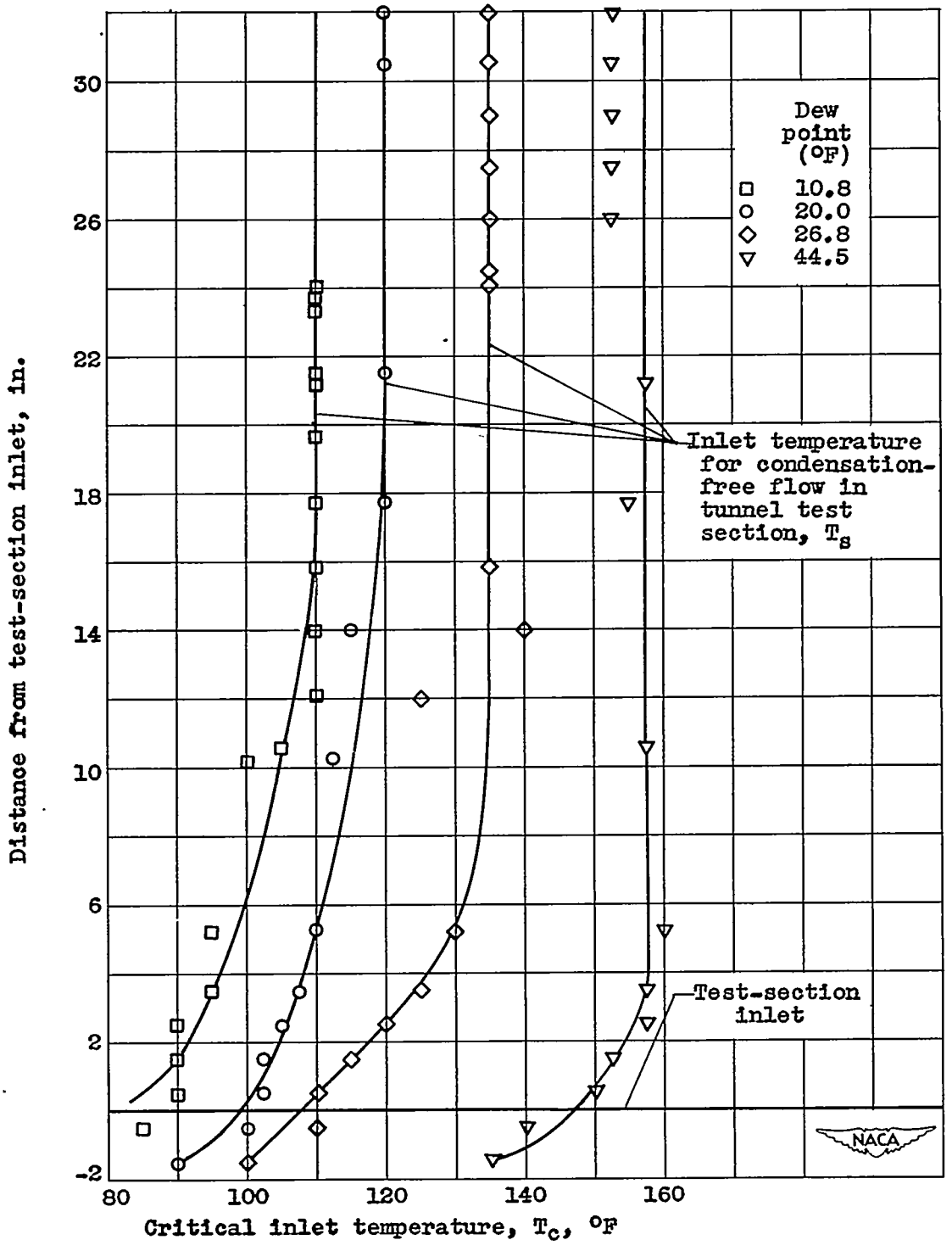

Figure 7. - Critical temperatures throughout test section of 3.4- by 3.4-inch tunnel. Mach number, 1.45.

1089

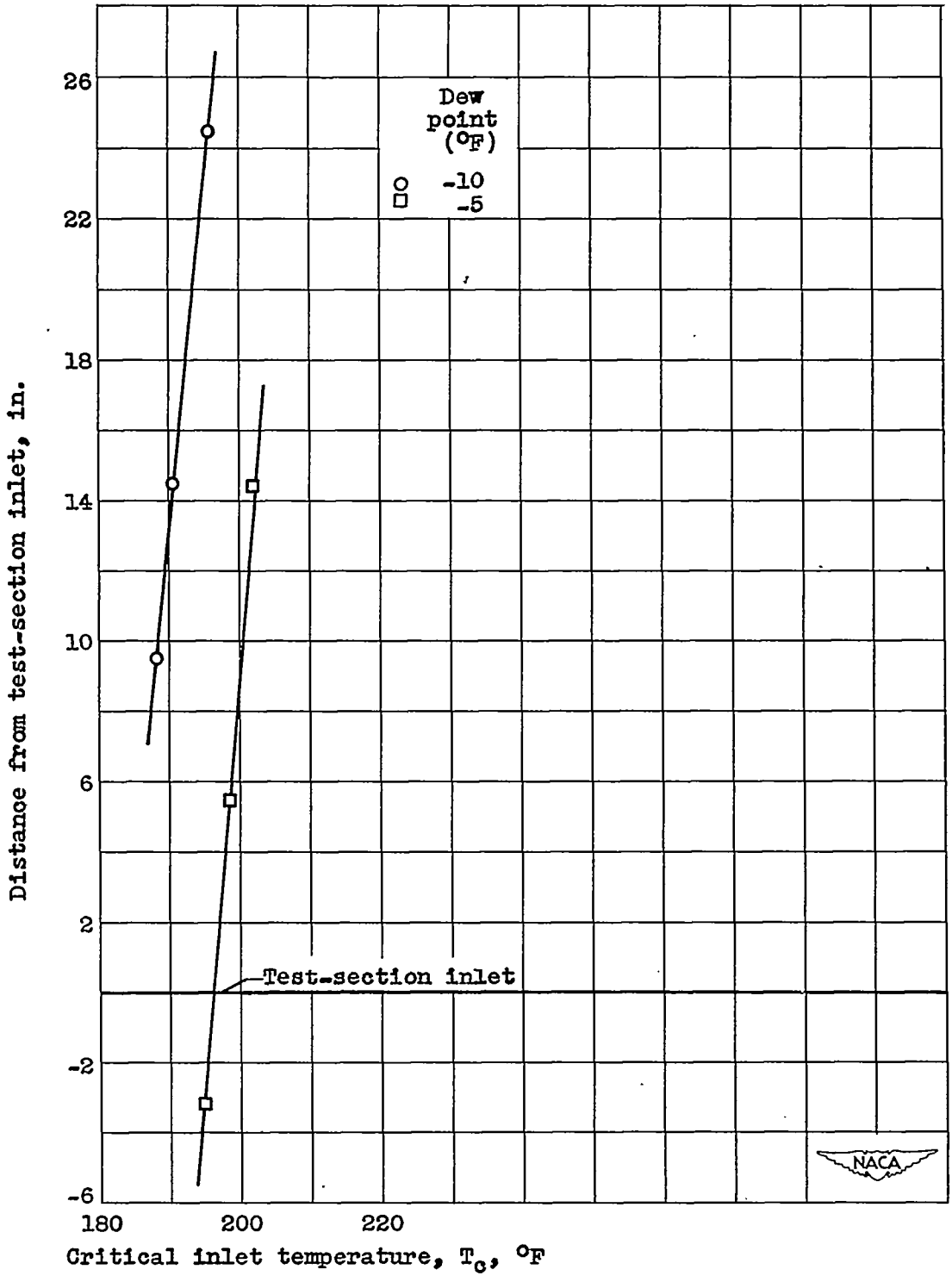

Figure 8. - Critical temperatures throughout test section of 4- by 10-inch tunnel. Mach number, 2.00.

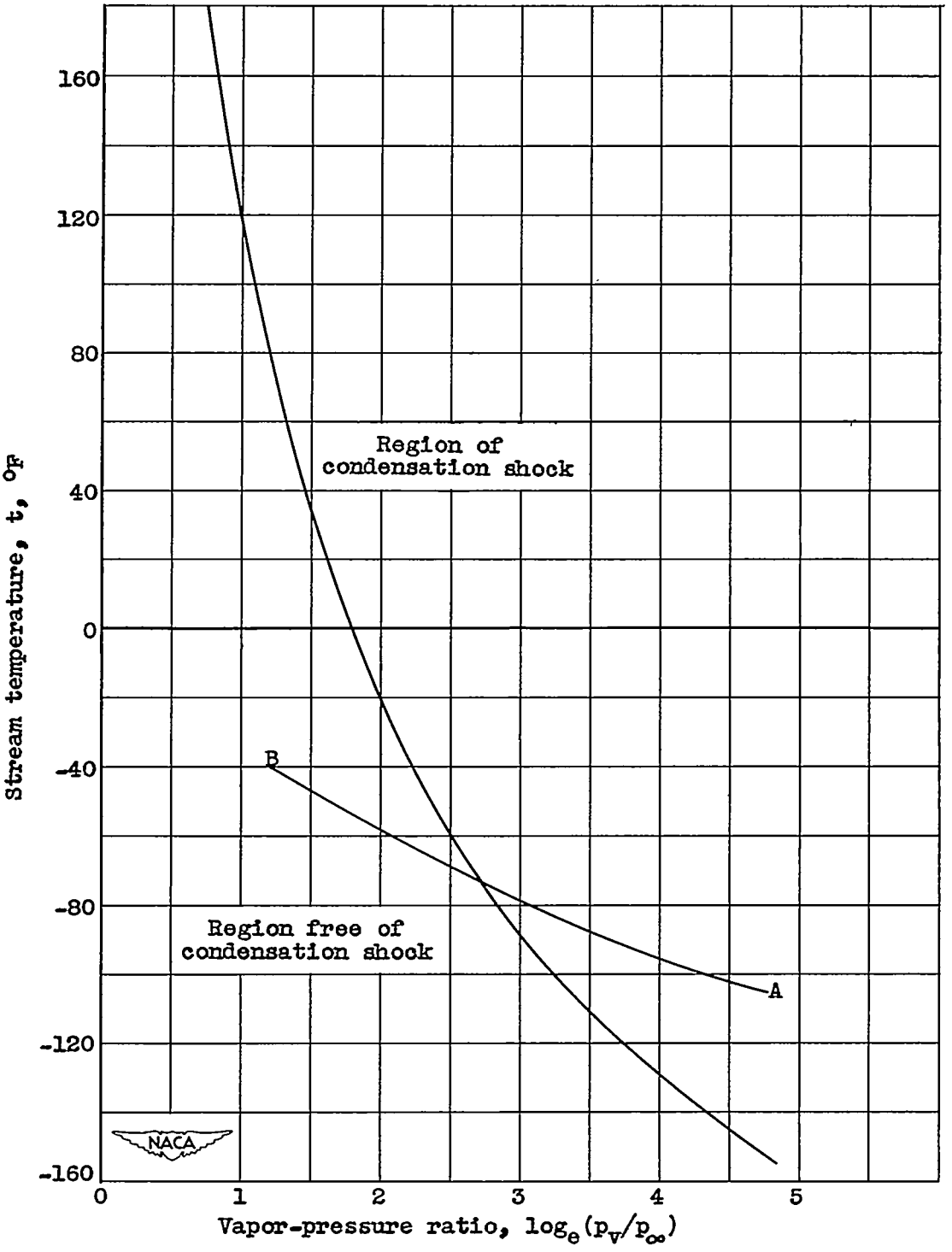

Figure 9. - Variation of stream temperature with vapor-pressure ratio. Log_e J, 4.1.

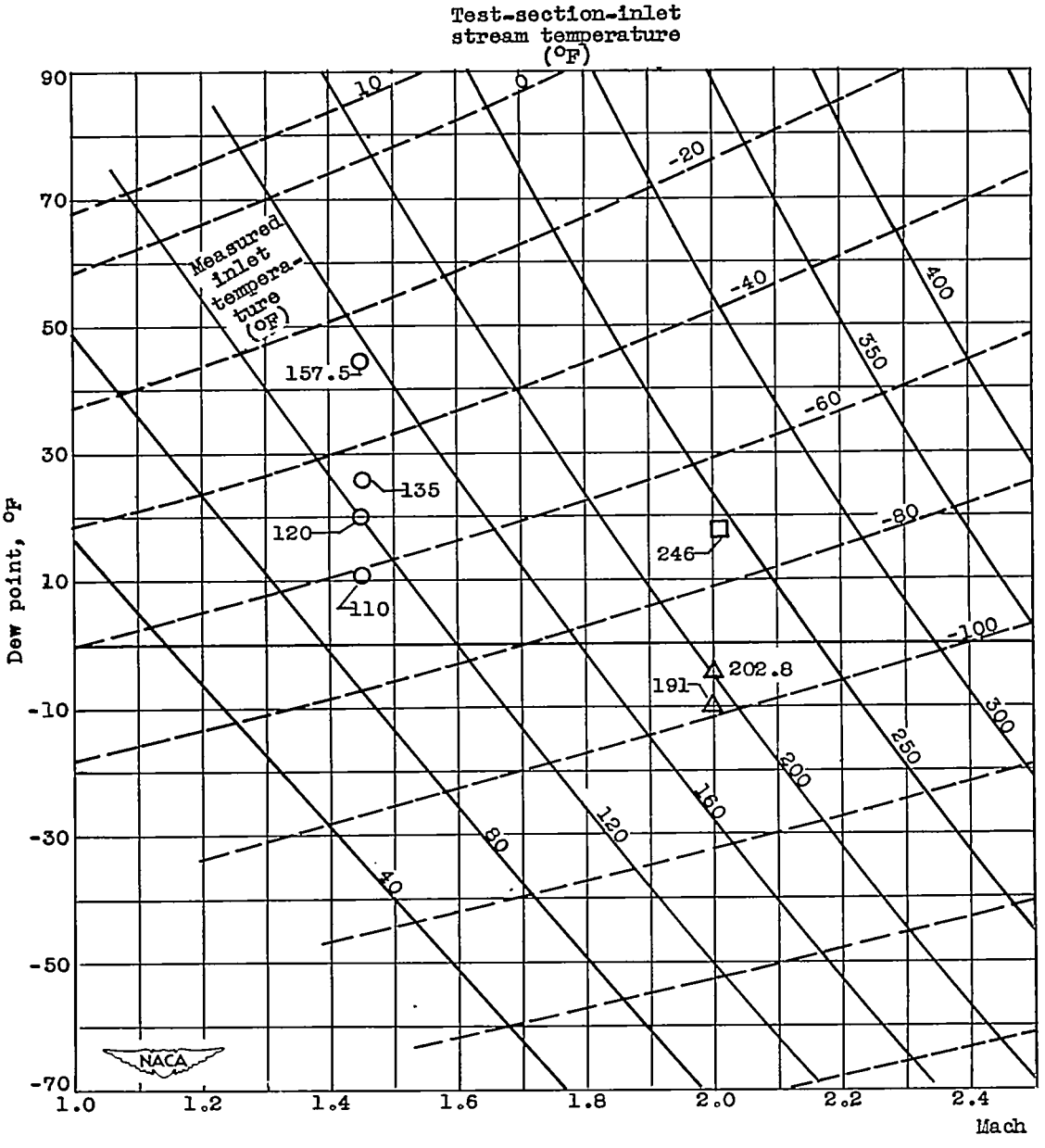

Figure 10. - Criterions for

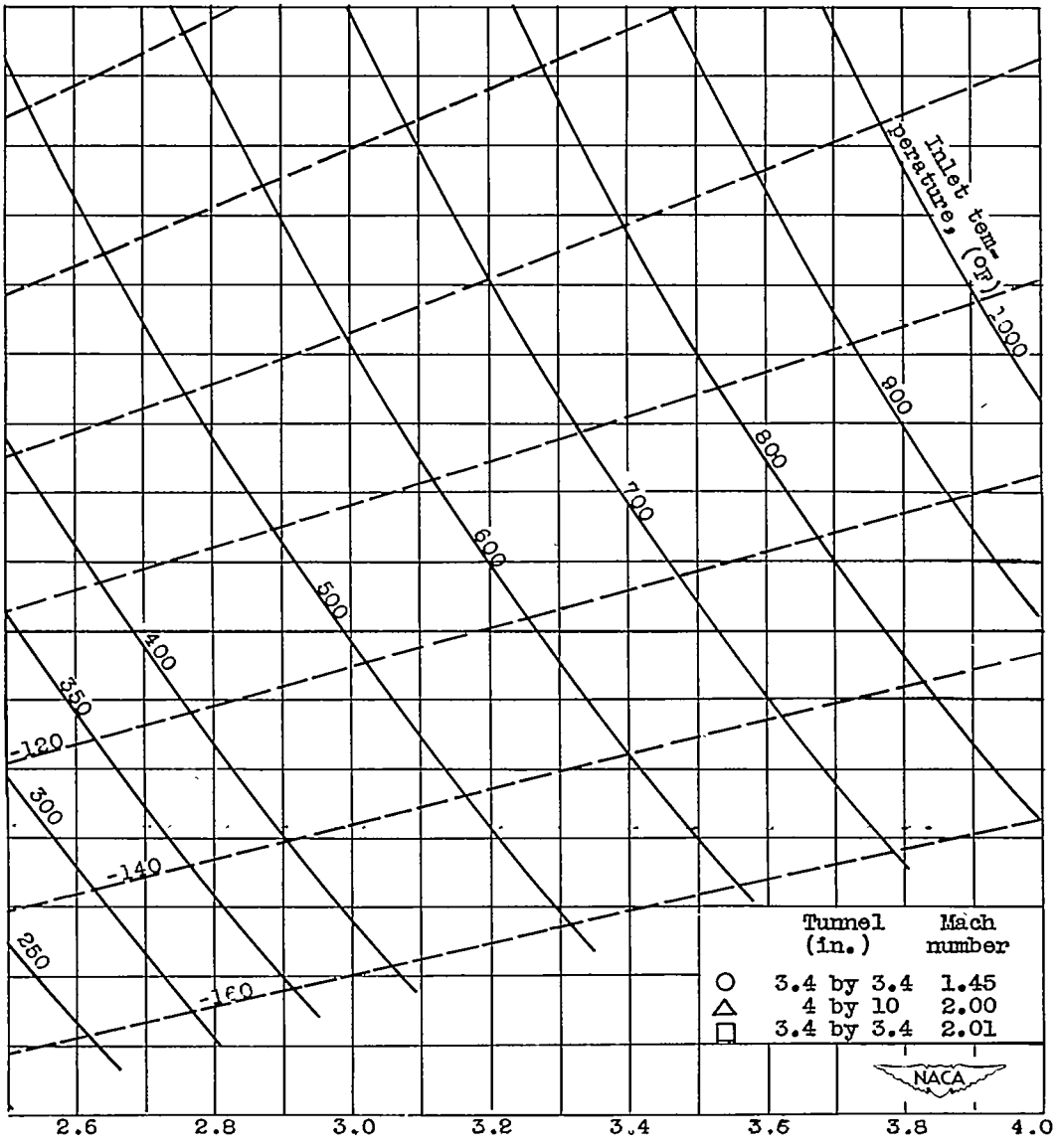

condensation-free flow.

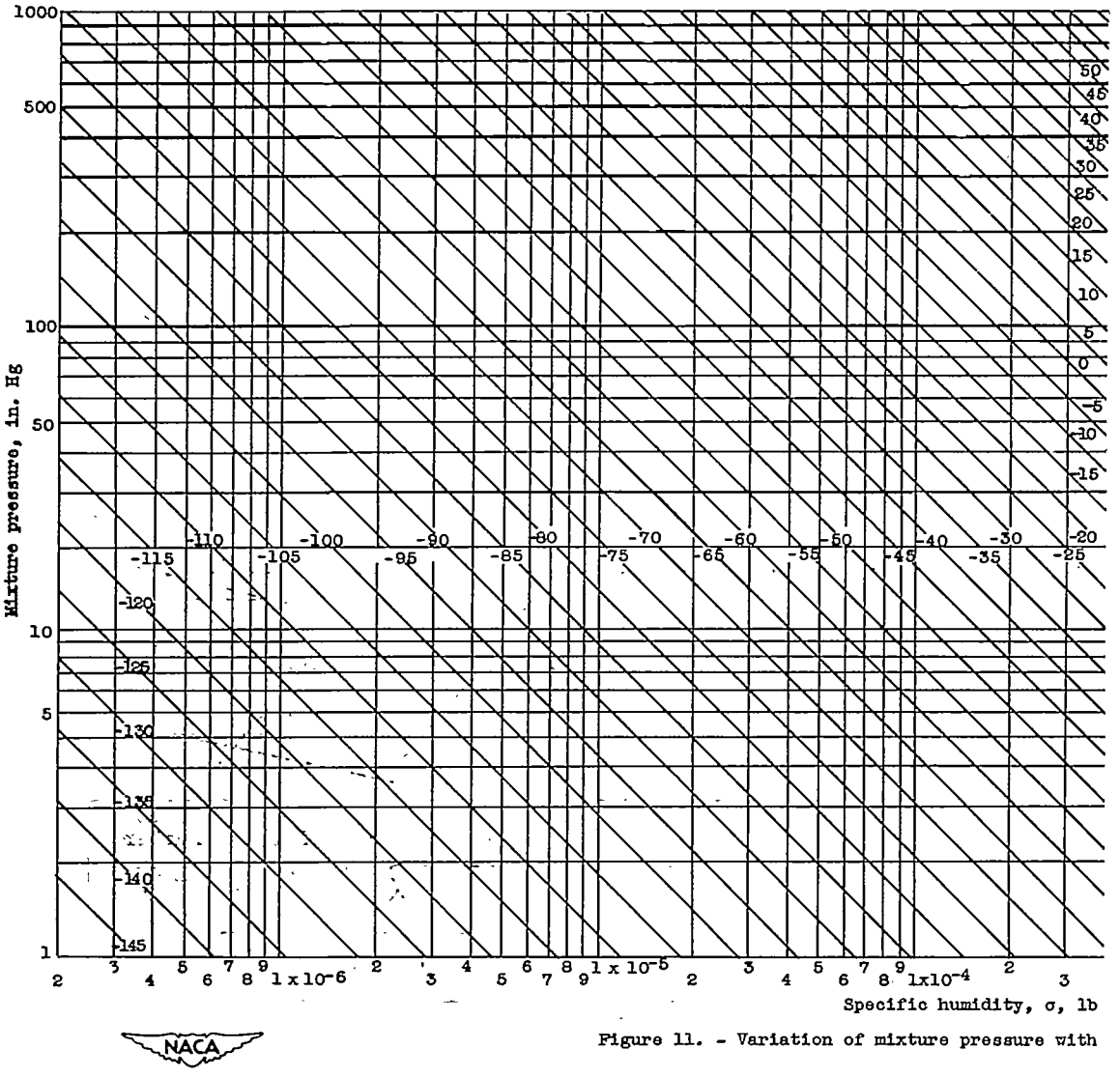

Figure 11. - Variation of mixture pressure with

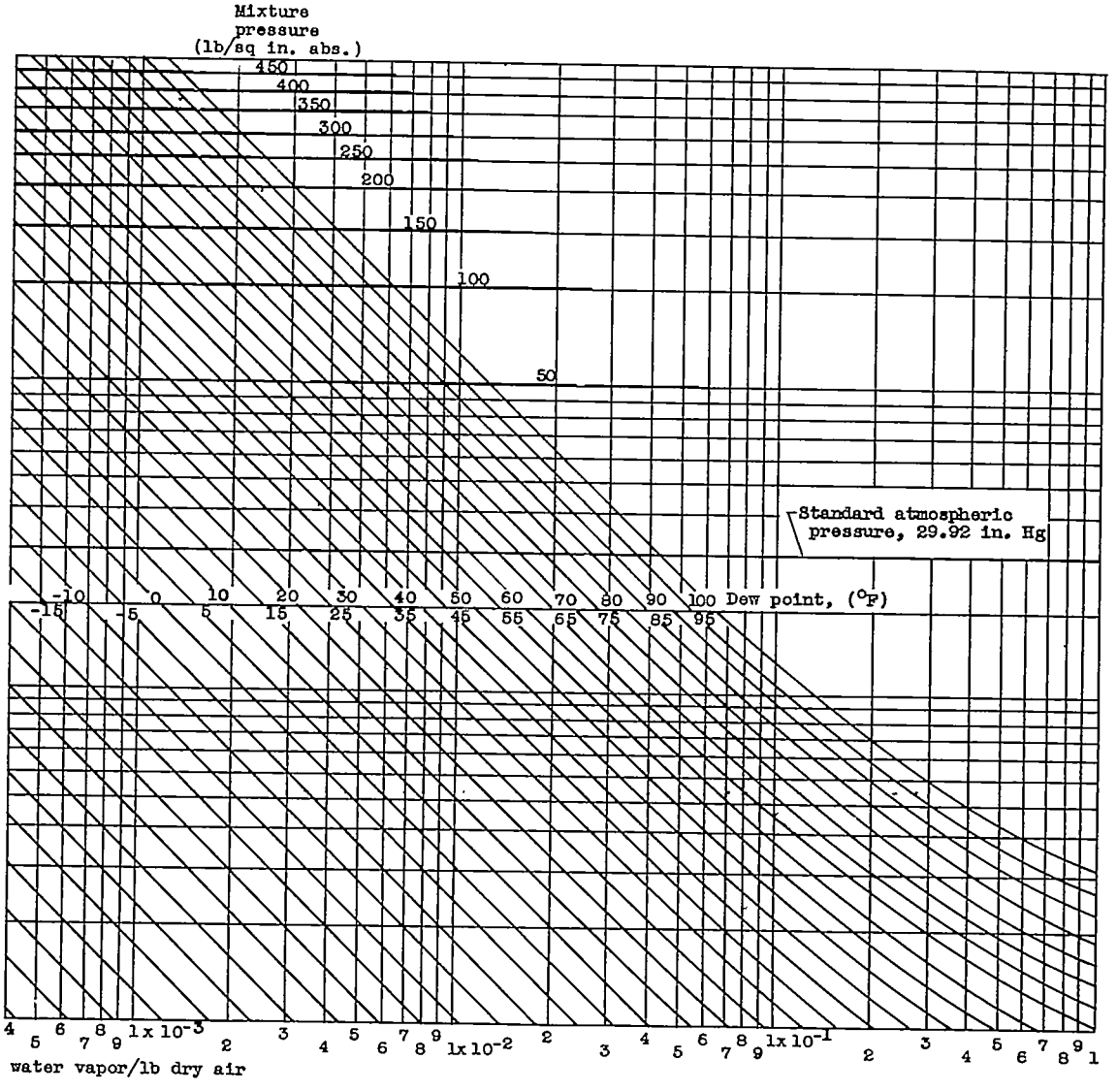

specific humidity for constant dew points.

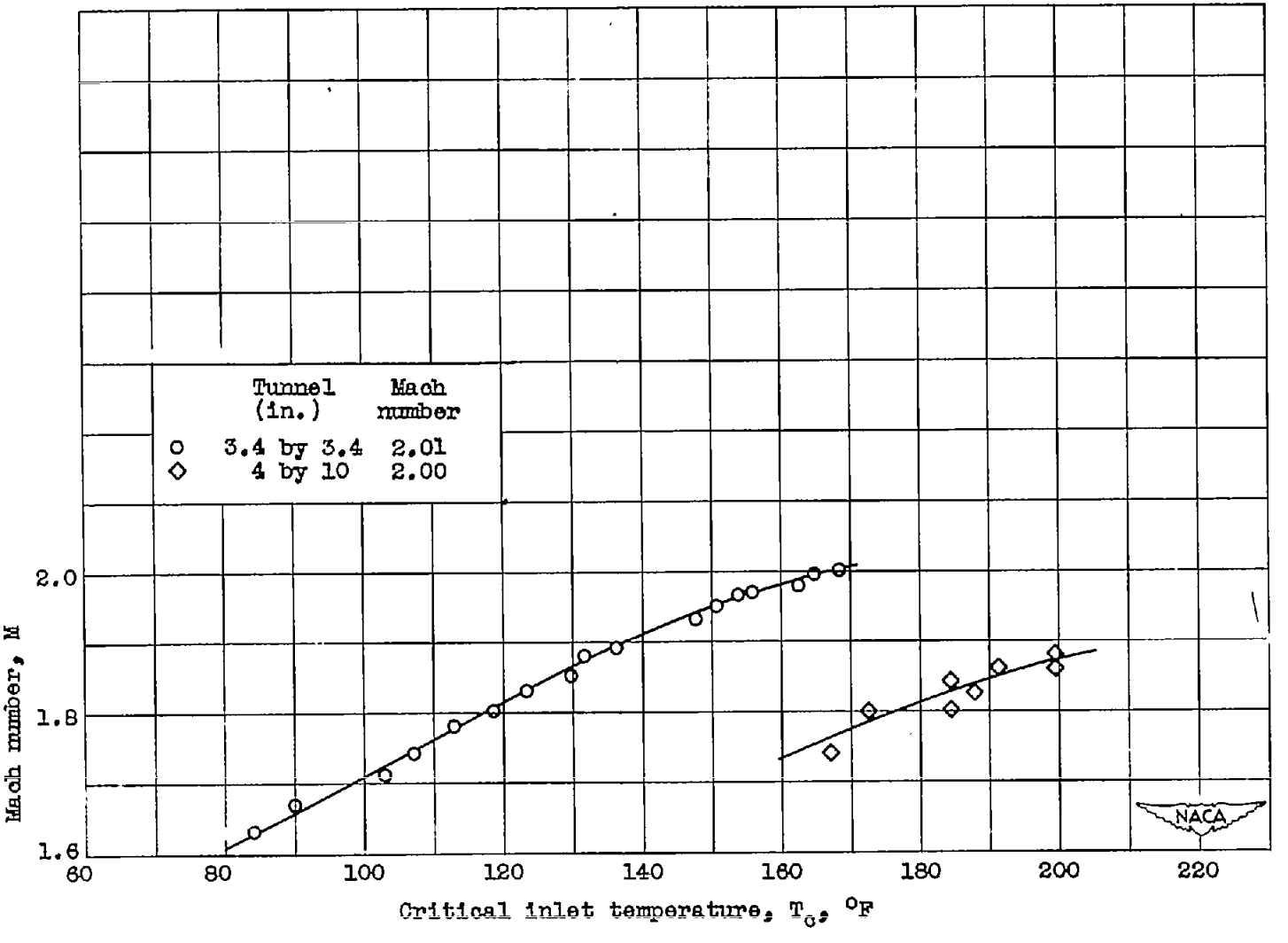

Figure 12. - Critical temperatures for various Mach numbers throughout nozzles of 3.4- by 3.4-inch and 4- by 10-inch tunnels at Mach numbers of 2.01 and 2.00, respectively. Dew point, 17.3° to 19.0° F.

Figure 13. - Ice formation in 3.4- by 3.4-inch tunnel. Mach number, 1.45; dew point, 70° F.

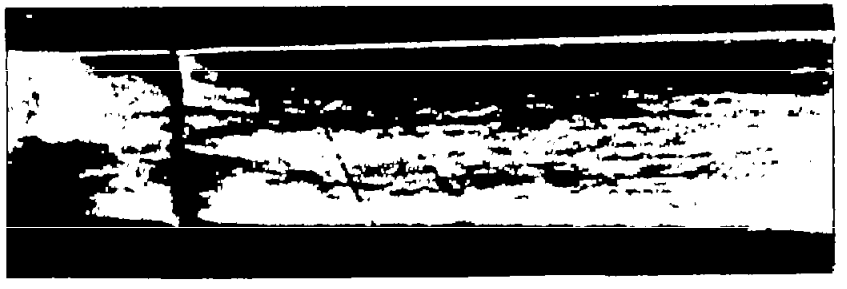

NACA
C-21438
5-14-48

(a) Condensation shock at throat in slowly diverging nozzle.

NACA
C-21436
5-14-48

(b) Condensation shock in figure 14(a) showing change in thickness with movement downstream.

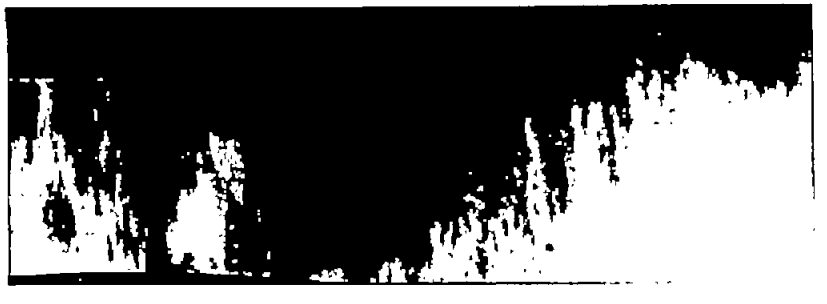

NACA
C-21434
5-14-48

(c) Condensation shock at throat in rapidly diverging nozzle.

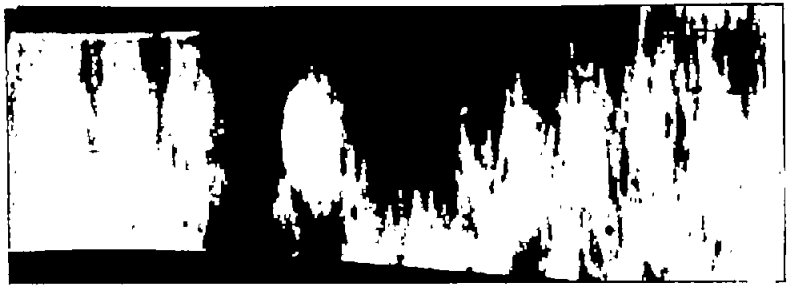

NACA
C-21439
5-14-48

(d) Condensation shock in figure 14(c) approaching conventional X-shape with movement downstream.

Figure 14. - Schlieren photographs of condensation shocks in supersonic flow in nozzles of 3.4- by 3.4-inch tunnel (flow from left to right).

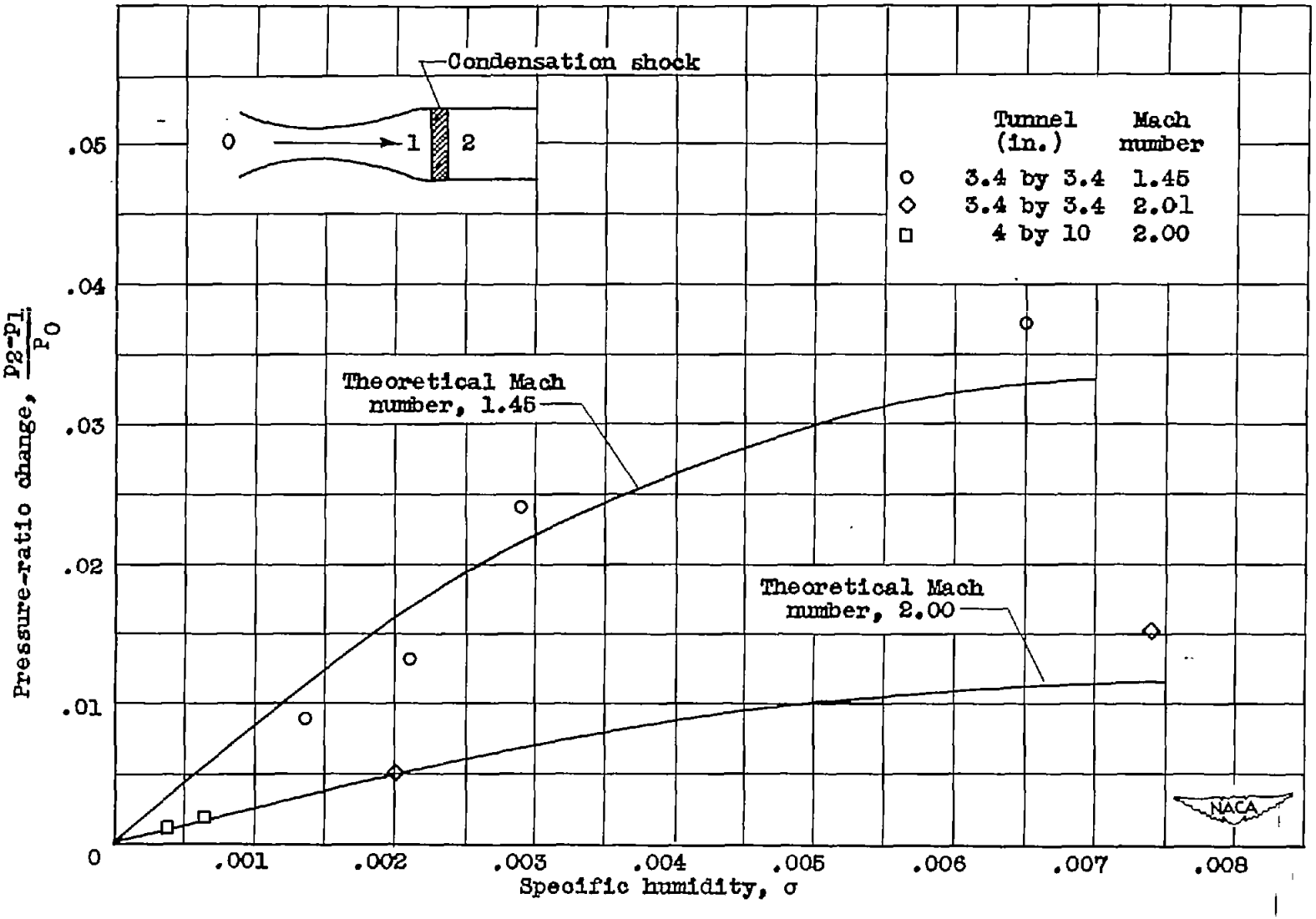

Figure 15. - Change in static-pressure ratio with specific humidity for condensation at Mach numbers 1.45 and 2.00